Nonequilibrium quantum criticality of interacting Dirac fermions

Yin-Kai Yu,[1] Zhi Zeng,[1] Zi-Xiang Li,[2,*] and Shuai Yin[1,†]

[1] *School of physics, Sun Yat-Sen University, Guangzhou 510275, China*
[2] *Beijing National Laboratory for Condensed Matter Physics & Institute of Physics, Chinese Academy of Sciences, Beijing 100190, China*

(Dated: April 11, 2023)

Investigating the impact of interacting Dirac fermions on quantum critical behavior is a crucial and challenging aspect of condensed matter theory. In this study, we introduce a comprehensive method for numerically examining nonequilibrium fermionic dynamics utilizing determinant quantum Monte Carlo (DQMC). We explore the imaginary-time relaxation dynamics of interacting Dirac fermions in the honeycomb Hubbard model. By employing initial states with either saturated antiferromagnetic (AF) order or disorder, we pinpoint the critical point and various critical exponents of this system through brief imaginary-time evolution processes, offering insights into previously contentious findings. Furthermore, we determine, for the first time, the initial slip exponent $\theta = -0.84(4)$ for the chiral Heisenberg universality class. Our approach enhances the efficiency of fermionic Monte Carlo calculations in general and presents a method for numerically studying nonequilibrium fermionic criticality. The potential of nonequilibrium fermion Monte Carlo in addressing the fermion sign problem is also discussed.

Introduction.— Dirac fermions as a type of low-energy excitation quasi-particle widely exists in various condensed matter systems, such as the highly studied graphene, d-wave superconductors, and gapless semiconductors[1–5]. Researchers have always been interested in the important role Dirac fermions play in novel universal critical phenomena. The Gross-Neveu theory predicted that interacting Dirac fermions can be divided into three Wilson-Fisher universality classes: chiral Heisenberg, chiral Ising, and chiral XY[6–12]. A most famous example is the coupling between massless Dirac fermions and Ising fields in the form of chiral mass to produce chiral Ising universality class (or Gross-Neveu-Yukawa universality class)[13–17]. Recently, one of us discovered that a new chiral tricritical point emerged when coupling Dirac fermions to a tricritical Ising model[18]. The common yet intriguing quantum criticality territory of Dirac fermions may serve as a stepping stone towards more universal quantum phase transition picture.

Studying Dirac fermions presents a significant challenge for theoretical analysis due to the interaction between fermions. Analytical work often relies on approximations or perturbations[6, 8, 18–22]. Determinant quantum Monte Carlo (DQMC) provides an unbiased method and a powerful tool for numerical studies of fermions. DQMC introduces auxiliary field degrees of freedom, which decouple many-body interactions into interactions between single-particle fermions and local auxiliary fields[23–26]. This allows the use of quantum Monte Carlo (QMC) methods to construct Markov chains of auxiliary field spacetime configurations for importance sampling. In recent years, DQMC has gained popularity as a tool for investigating the ground-state characteristics of Dirac fermion systems. It has been successful in demonstrating equilibrium quantum criticality in these systems[27–32]. The typical approach to solving the ground state involves creating an initial trial wave function and then projecting it onto the ground state through imaginary-time evolution operators simulated by DQMC. After a long period of imaginary time evolution, only information about the thermal ground state is obtained.

However, they ignores important prethermal information related to fermionic quantum criticality that is hidden in the initial state and imaginary time evolution process. According to dynamic scaling theory, this neglected prethermal information not only sufficiently demonstrates all thermal criticalities of fermions but also includes nonequilibrium criticalities unique to prethermal, such as memory effects on the initial state[22, 33–40]. Moreover, nonequilibrium criticality exhibited by DQMC simulated imaginary time dynamics can be observed in real-time dynamic experiments, and direct imaginary time dynamic experiments have already been preliminarily implemented in quantum computers[41–50]. Therefore, we are strongly motivated to extend DQMC that shines brightly in equilibrium fermionic quantum criticality research into the nonequilibrium field.

This study for the first time extends DQMC for calculating fermionic nonequilibrium quantum criticality. We also demonstrated for the first time the nonequilibrium initial slip critical exponent of interacting Dirac fermions' chiral Heisenberg universality class. Specifically, we studied half-filled honeycomb Hubbard model with SU(2) symmetry at its critical point's imaginary time relaxation dynamics. The model is the most popular interacting Dirac fermion model but there was still no consensus on its phase transition behavior from previous equilibrium studies[8, 21, 27, 32]. Unlike equilibrium methods where arbitrary trial wave functions are selected as initial states, we chose specific initial states and observed

their imaginary time evolution processes at phase transition points instead of just studying ground states. With this nonequilibrium method that fully utilizes prethermal information, we determined system's phase transition critical point and universal critical exponents with fewer computational resources while also calculating an initial slip exponent characterizing memory effects on the initial state. Finally, we mention potential applications of this method to address fermion sign problems.

Model.— We consider the finite-sized two-dimensional spin-$\frac{1}{2}$ Hubbard model on a half-filled honeycomb lattice. The Hamiltonian reads

$$H = -t \sum_{\langle ij\rangle,\sigma} c_{i\sigma}^{\dagger} c_{j\sigma} + U \sum_{i} \left(n_{i\uparrow} - \frac{1}{2}\right)\left(n_{i\downarrow} - \frac{1}{2}\right), \quad (1)$$

in which $c_{i\sigma}^{\dagger}$ ($c_{j\sigma}$) represents the creation (annihilation) operator of spin $\sigma =\uparrow,\downarrow$ electrons, $n_{i\sigma} = c_{i\sigma}^{\dagger} c_{i\sigma}$ is the electron number operator on site i, and the summation index $\langle ij\rangle$ only sums over nearest neighbor sites. The coefficient t is the hopping amplitude, and U is the Coulomb repulsion potential. In the strong coupling limit $U/t \gg 1$ (weak coupling limit $U/t \ll 1$), the system tends to exhibit antiferromagnetic Mott insulator phase (Dirac semimetal phase)[32]. During the phase transition, the energy gap closes at Dirac points and shows features of interacting massless Dirac fermions. In the strong coupling regime, this model can be map into a chiral Heisenberg model through Schrieffer-Wolff transformation[51]. The quamtum criticality of chiral Heisenberg universality class play a role near this renormalization fixed point.

Method.— We employ the large-scale determinant quantum Monte Carlo (DQMC) method [26] to investigate the imaginary-time relaxation dynamics of our model. Specifically, we prepare a specific initial state $|\psi_0\rangle$ and set the system parameters U/t on the critical point to observe the scaling behavior of observables during the prethermal stage. When the system evolves to imaginary time τ (less than relaxation time ζ), the expectation value of observables is given by

$$\langle O(\tau)\rangle = \frac{\langle\psi_0|\, \mathrm{e}^{\tau H/2}\, O\, \mathrm{e}^{\tau H/2}\, |\psi_0\rangle}{\langle\psi_0|\, \mathrm{e}^{\tau H}\, |\psi_0\rangle}. \quad (2)$$

In numerical calculations, we use Trotter decomposition [52] to discretize imaginary-time propagator into $M = \tau/\Delta\tau$ (M is integer) time slices with $\mathrm{e}^{H\tau} = \left(\mathrm{e}^{\Delta\tau H_t}\mathrm{e}^{\Delta\tau H_U} + \mathcal{O}\left(\Delta\tau^2\right)\right)^M$, where H_t and H_U are the hopping term and Hubbard interaction term respectively in the Hamiltonian (Eq. (1)). We choose small enough $\Delta t/t < 0.05$. To decouple two-body fermion-fermion coupling form of $\mathrm{e}^{\Delta\tau H_U}$, we use a discrete Hubbard-Stratonovich transformation to obtain one-body fermion-auxiliary field coupling. Here, we introduce a four-component space-time local auxiliary fields[53], and use DQMC for importance sampling over these space-time configurations. More details used here are similar to those employed when solving thermal ground states as described in Ref. [26]. Due to the bipartite structure of honeycomb, there is no sign problem encountered during this process [54].

Critical point calculated by prethermal methods.— Considering the ongoing controversy surrounding the determination of critical points based on equilibrium studies, we present nonequilibrium information to establish the critical point of phase transition. Focusing on the dependence of the antiferromagnetization (AF) on system parameters, we use DQMC to calculate the antiferromagnetic structure factor[29, 32]

$$S(\boldsymbol{q}) = \frac{1}{L^2}\sum_{i,j} \mathrm{e}^{\mathrm{i}\boldsymbol{q}\cdot(\boldsymbol{r}_i - \boldsymbol{r}_j)} \langle m_i^{(z)} m_j^{(z)}\rangle. \quad (3)$$

Here, staggered magnetization $m_i^{(z)}$ is defined as: $m_i^{(z)} = \vec{c}_{i,A}^{\dagger}\sigma^z\vec{c}_{i,A} - \vec{c}_{i,B}^{\dagger}\sigma^z\vec{c}_{i,B}$. where i is the index of unit cell, A and B represent different sublattices, and Pauli-z matrix σ^z acting on the spin degree of freedom $\vec{c} = (c_\uparrow, c_\downarrow)$. We define correlation ratio R as[29]

$$R = S(\mathbf{0})/S(\Delta\boldsymbol{q}), \quad (4)$$

where $\Delta\boldsymbol{q} = \left(\frac{1}{L}\boldsymbol{b}_1 + \frac{1}{L}\boldsymbol{b}_2\right)$ is minimum lattice momentum. The correlation ratio is dimensionless. We set initial state to saturated AF, and near the equilibrium critical point, correlation ratio follows universal scaling form given by[34]

$$R(g,\tau,L) = f_R\left(gL^{1/\nu}, \tau^{-1}L^z\right), \quad (5)$$

where $g = (U - U_c)/t$ represents distance between system parameters and critical point, usually $t = 1$. For Dirac fermions, dynamic critical exponent $z = 1$.

Here we fix $\tau^{-1}L^z$, so the correlation ratio at the critical point $g = 0$ is independent of size. As shown in Fig. 1, we calculate the correlation ratio $R(U/t)$ as a function of Hubbard parameter for different sizes, and identify the intersection points $(U/t)^{\times}$ between curves for sizes L and $L+3$ as pseudo-critical points for size L. We use an extrapolation form of $(U/t)^{\times} = a + bL^{-\omega}$ to obtain the thermodynamic limit value $U/t = 3.91 \pm 0.03$ of critical point at fixed $\tau/L = 0.3$. This result will be used in the following quantum criticality analysis. The results with fixed values of $\tau/L = 0.34, 0.5$, also shown in Fig. 1, extrapolate to the same critical point within error range, thus demonstrating that our method based on nonequilibrium information to determine critical points using dynamic scaling Eq. (4) is reliable.

The relaxation dynamics-based method we used above to solve the critical point can be applied universally to other fermion systems. Nevertheless, it is worth mentioning that as shown in Fig. 1(b), the pseudo-critical point $(U/t)^{\times}$ approaches the critical point with different

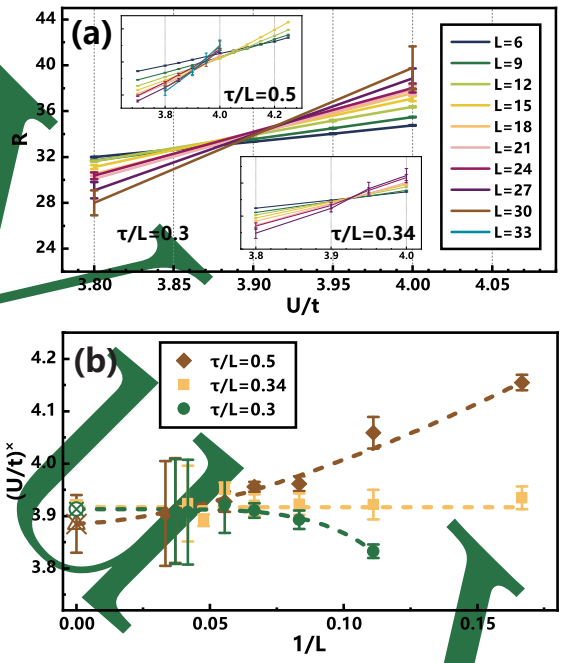

FIG. 1. Correlation ratio curves $R(U/t)$ of different sizes L intersect at the critical point. (a) shows the curves of $R(U/t)$ when $\tau/L = 0.3, 0.34, 0.5$ are fixed respectively. (b) extracts the intersection points $(U/c)^{\times}$ of adjacent size's $R(U/t)$ curves from (a), and shows how these intersection points change with $1/L$. The critical point is extrapolated when the system tends to thermodynamic limit $L \to \infty$. The extrapolation result for $\tau/L = 0.3$ is $U/t = 3.91 \pm 0.03$, for $\tau/L = 0.34$ it is $U/t = 3.92 \pm 0.01$, and for $\tau/L = 0.5$ it is $U/t = 3.89 \pm 0.05$. Note that the extrapolation results are also marked at $1/L = 0$ in (b).

trends as L increases when different values of τ/L are taken. Specifically, when $\tau/L = 0.3$, the pseudo-critical point under small size is smaller than the true critical point at thermodynamic limit; while when $\tau/L = 0.5$, the pseudo-critical point under small size is larger than the true critical point; even more interestingly, we found that at $\tau/L = 0.34$, the pseudo-critical point almost does not depend on size and can exhibit a real critical behavior under small sizes alone. We have not yet observed universality of this novel phenomenon resulting from coupling finite size and time effects in other two-ordered fermionic phase transitions. Our preliminary understanding suggests that due to disorder of Dirac semimetal in short-time stage, fermion fluctuations have a greater impact while opposite holds true in near-equilibrium stage. This phenomenon may even suggest new methods for finding critical points through finite size-time effects by determining special moments like $\tau/L = 0.34$ based on judging trend of pseudo-critical points but further discussion will be omitted here.

Relaxation dynamics.— After identifying the critical point, we use DQMC to simulate the relaxation dynamics at our critical point. As a demonstration, we show how to use nonequilibrium methods to determine the critical exponents of fermionic universality classes, which have already been calculated in many equilibrium studies but with some results still showing significant differences[27, 28, 32]. Here, we calculate the square of AF order parameter as

$$m^2 = S(\mathbf{0}), \tag{6}$$

where $S(\mathbf{0})$ is the AF structure factor at zero momentum and is calculated by Eq. (3). We set initial states for imaginary time evolution as both AF disordered ($m_0 = 0$) and AF saturated ($m_0 = 1$), respectively, by solving eigenstates of pure hopping Hamiltonian and pure AF Hamiltonian. In this case, relaxation process of squared order parameter m^2 at critical point $g = 0$ follows finite-size scaling given by

$$m^2 = L^{2\beta/\nu} f_{m^2}\left(\tau^{-1} L^z\right), \tag{7}$$

where f_{m^2} is a universal scaling function independent of system size. In Fig. 2(a), we present relaxation behavior of $m^2(\tau)$ under different sizes. We rescale them according to Eq. (7), fitting that all relaxation curves collapse into universal functional form f_{m^2}. yielding ratio between critical exponents $\beta/\nu = 0.80 \pm 0.03$. This yields a ratio between critical exponents $\beta/\nu = 0.80 \pm 0.03$. In Fig. 2(b), we verify the universality of our results.

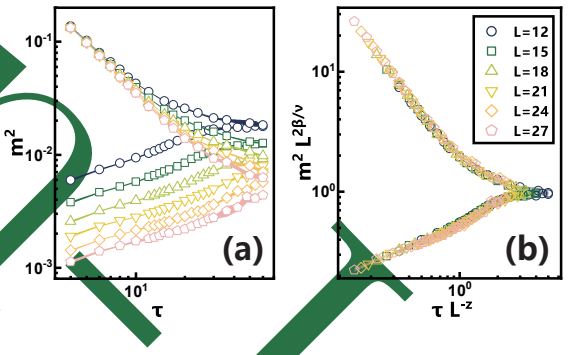

FIG. 2. The relaxation of the antiferromagnetic order parameter $m^2(\tau)$ and its rescaling. (a) shows the relaxation curves of different sizes, size labeling consistent with (b). The rising curve represents an initial disordered state, while the falling curve represents an initial saturated state. The relaxation curves in (b) are rescaled according to critical exponents $\beta/\nu = 0.80$, and the curves of different sizes overlap. The line width is equal to the error bar.

Initial slip exponent.— We for the first time determine the initial slip exponent θ of chiral Heisenberg universality class. This important critical exponent characterizes the memory of order parameter with respect to the initial state, and has real-time observable effects[18, 22, 55–57]. To obtain θ, we define imaginary-time correlation as[37]

$$A = \frac{1}{L^2} \sum_i \langle m_i^{(z)}(0)\, m_i^{(z)}(\tau) \rangle, \tag{8}$$

where index i sums over all unit cells. $m_i^{(z)}(0)$ is a local staggered magnetization operator at initial time, which has the same dimension as the initial AF order parameter $m_0 \sim L^{-x_0}$. In a complete finite-size scaling analysis, Eq. (5) and Eq. (7) should include dimensionless variable $m_0 L^{x_0}$, but our choice of initial state allows us to neglect this variable. According to definition Eq. (8) and $m_i \sim L^{-\beta/\nu}$, we can derive that A scales as $A \sim L^{x_0-\beta/\nu-d}$ where system dimension $d = 2$. Using scaling law[57]

$$x_0 = \theta z + \beta/\nu, \tag{9}$$

we obtain universal scaling

$$A = L^{\theta z - d} f_A\left(\tau^{-1} L^z\right). \tag{10}$$

The universality in this equation depends on critical point $g = 0$ and random up-down initial state with disorder $m_0 = 0$. This means that besides Monte Carlo averaging, we also need to average over different samples of initial states numerically which greatly increases computational cost. Efficient nonequilibrium calculations enable us to obtain good results nonetheless. We show in Fig. 3 relaxation behavior of imaginary-time correlation $A(\tau)$, and control θ so that rescaled curves perfectly overlap in Eq. (10) form. From this, we determine the initial slip exponent $\theta = -0.84 \pm 0.04$, whose accuracy is verified by the overlap in Fig. 3.

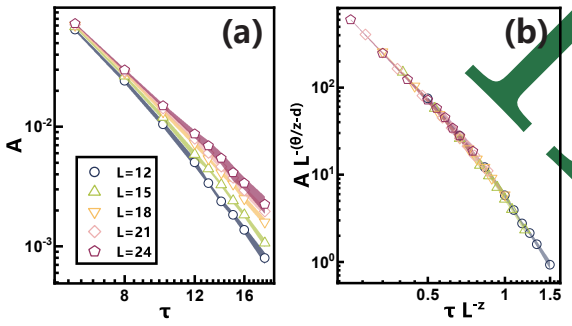

FIG. 3. The relaxation of the imaginary-time correlation $A(\tau)$ and its rescaling. (a) shows the relaxation curves of different sizes. The relaxation curves in (b), size labeling consistent with (a), are rescaled according to critical exponents $\theta = -0.84$, and the curves of different sizes overlap. The line width is equal to the error bar.

Discussion and conclusion.— In studying the nonequilibrium criticality of interacting fermions, we adopt a universal approach. This involves preparing specific initial states and simulating the system's imaginary-time evolution through DQMC. We then calculate observables based on equal-time Green's functions and study the scaling behavior of the system's relaxation dynamics. In this work, we demonstrate a specific methodology and results for applying this universal method to the interacting Dirac fermion system.

In our method, we do not need to go through a long wait until the system reaches equilibrium. We can obtain all critical exponents of the system and accurately predict its critical behavior in equilibrium state through a short imaginary time evolution process. The introduction of this method may significantly improve the efficiency of numerical studies on fermions and save computational resources. For the Hubbard model in honeycomb lattice, we compare our results with previous research results in Table. I. Considering that there is still no consensus on the critical point and critical exponents of this model in past results, our results can also serve as a new reference.

TABLE I. Quantum criticality of honeycomb Hubbard and chiral Heisenberg universality class. The first row of data in the table shows the numerical results obtained by our work through nonequilibrium fermion Monte Carlo methods. The remaining rows display related research findings for comparison purposes. In the table, honeycomb refers to the Hubbard model on a honeycomb lattice. It is important to note that our method is unique in its ability to calculate the nonequilibrium critical exponent θ.

model	method	U_c/t	β/ν	θ
honeycomb	QMC (non-EQ)	3.91(3)	0.80(3)	−0.84(4)
honeycomb	QMC[32]	3.85(2)	0.75(2)	-
honeycomb	QMC[27]	3.77(4)	0.9(1)	-
Gross-Neveu	$4-\epsilon$ (1st order)[8]	-	0.945	-
Gross-Neveu	$4-\epsilon$ (2nd order)[8]	-	0.985	-
Gross-Neveu	FRG[21]	-	1.008	-

Moreover, this work opens up a universal path for studying nonequilibrium criticality in interacting fermionic systems. By controlling the given initial state, our method can investigate the influence of the initial state on imaginary time evolution. We have determined the initial slip exponent for chiral Heisenberg universality class in interacting fermionic systems to be $\theta = -0.84 \pm 0.04$.

Nevertheless, our nonequilibrium approach has the potential to address the challenging fermion sign problem, which has hindered progress in numerically studying fermionic systems[15, 58]. This problem arises during simulations of imaginary-time evolution of fermions and can result in negative weights in Monte Carlo sampling, rendering importance sampling ineffective. However, our method requires only a short imaginary time evolution to predict critical behavior of the system, potentially enabling us to overcome this limitation. Our future work will focus on exploring this direction.

Acknowledgement: This work is supported by (national) college students innovation and entrepreneurship training program, Sun Yat-sen University.

* zixiangli@iphy.ac.cn
† ymsh6@mail.sysu.edu.cn

[1] K. S. Novoselov, A. K. Geim, S. V. Morozov, D.-e. Jiang, Y. Zhang, S. V. Dubonos, I. V. Grigorieva, and A. A. Firsov, Electric field effect in atomically thin carbon films, science **306**, 666 (2004).
[2] Y. Zhang, Y.-W. Tan, H. L. Stormer, and P. Kim, Experimental observation of the quantum hall effect and berry's phase in graphene, nature **438**, 201 (2005).
[3] M. Z. Hasan and C. L. Kane, Colloquium: topological insulators, Reviews of modern physics **82**, 3045 (2010).
[4] S. Murakami, Phase transition between the quantum spin hall and insulator phases in 3d: emergence of a topological gapless phase, New Journal of Physics **9**, 356 (2007).
[5] C. C. Tsuei and J. R. Kirtley, Pairing symmetry in cuprate superconductors, Rev. Mod. Phys. **72**, 969 (2000).
[6] D. J. Gross and A. Neveu, Dynamical symmetry breaking in asymptotically free field theories, Physical Review D **10**, 3235 (1974).
[7] K. G. Wilson and M. E. Fisher, Critical exponents in 3.99 dimensions, Phys. Rev. Lett. **28**, 240 (1972).
[8] B. Rosenstein, Hoi-Lai Yu, and A. Kovner, Critical exponents of new universality classes, Physics Letters B **314**, 381 (1993).
[9] H. Gies and C. Wetterich, Renormalization flow of bound fermion states, Physical Review D **71**, 095006 (2005).
[10] I. F. Herbut, Interacting electrons in graphene: Fermi velocity renormalization and effective four-fermion interaction, Physical Review B **79**, 085116 (2009).
[11] Y. Nambu and G. Jona-Lasinio, Dynamical model of elementary particles based on an analogy with superconductivity. i, Phys. Rev. **122**, 345 (1961).
[12] Y. Nambu and G. Jona-Lasinio, Dynamical model of elementary particles based on an analogy with superconductivity. ii, Phys. Rev. **124**, 246 (1961).
[13] J. Zinn-Justin, *Quantum field theory and critical phenomena*, Vol. 171 (Oxford university press, 2021).
[14] T.-T. Wang and Z. Y. Meng, Emus live on the gross-neveu-yukawa archipelago (2023), arXiv:2304.00034 [cond-mat.str-el].
[15] Z.-X. Li, Y.-F. Jiang, and H. Yao, Fermion-sign-free Majarana-quantum-Monte-Carlo studies of quantum critical phenomena of Dirac fermions in two dimensions, New Journal of Physics **17**, 085003 (2015).
[16] Y.-F. Jiang, Z.-X. Li, S. A. Kivelson, and H. Yao, Charge-4*e* superconductors: A majorana quantum monte carlo study, Phys. Rev. B **95**, 241103 (2017).
[17] Z.-X. Li, Y.-F. Jiang, and H. Yao, Solving the fermion sign problem in quantum monte carlo simulations by majorana representation, Phys. Rev. B **91**, 241117 (2015).
[18] S. Yin, S.-K. Jian, and H. Yao, Chiral Tricritical Point: A New Universality Class in Dirac Systems, Physical Review Letters **120**, 215702 (2018).
[19] K. G. Wilson, The renormalization group: Critical phenomena and the kondo problem, Rev. Mod. Phys. **47**, 773 (1975).
[20] J. Polchinski, Effective field theory and the fermi surface, arXiv preprint hep-th/9210046 (1992).
[21] L. Janssen and I. F. Herbut, Antiferromagnetic critical point on graphene's honeycomb lattice: A functional renormalization group approach, Phys. Rev. B **89**, 205403 (2014).
[22] S.-K. Jian, S. Yin, and B. Swingle, Universal Prethermal Dynamics in Gross-Neveu-Yukawa Criticality, Physical Review Letters **123**, 170606 (2019).
[23] R. Blankenbecler, D. J. Scalapino, and R. L. Sugar, Monte carlo calculations of coupled boson-fermion systems. i, Phys. Rev. D **24**, 2278 (1981).
[24] J. E. Hirsch, Two-dimensional hubbard model: Numerical simulation study, Phys. Rev. B **31**, 4403 (1985).
[25] F. Assaad and H. Evertz, World-line and determinantal quantum monte carlo methods for spins, phonons and electrons, in *Computational Many-Particle Physics* (Springer Berlin Heidelberg, Berlin, Heidelberg, 2008) pp. 277–356.
[26] F. F. Assaad, Quantum monte carlo methods on lattices: The determinantal approach, Quantum Simulations of Complex Many-Body Systems: From Theory to Algorithms **10**, 99 (2002).
[27] F. F. Assaad, F. Parisen Toldin, M. Hohenadler, and I. F. Herbut, Fermionic quantum criticality in honeycomb and π-flux Hubbard models: Finite-size scaling of renormalization-group-invariant observables from quantum Monte Carlo, Physical Review B **91**, 165108 (2015).
[28] F. F. Assaad and I. F. Herbut, Pinning the Order: The Nature of Quantum Criticality in the Hubbard Model on Honeycomb Lattice, Physical Review X **3**, 031010 (2013).
[29] S. Sorella, Y. Otsuka, K. Seki, and S. Yunoki, Dirac electrons in the square lattice Hubbard model with a *d*-wave pairing field: chiral Heisenberg universality class revisited, Physical Review B **102**, 235105 (2020), arXiv:2009.04685 [cond-mat].
[30] S. Sorella, K. Seki, Y. Otsuka, and S. Yunoki, Fermi-liquid ground state of interacting Dirac fermions in two dimensions, Physical Review B **99**, 125145 (2019).
[31] S. Sorella, Y. Otsuka, K. Seki, and S. Yunoki, Quantum criticality in the metal-superconductor transition of interacting Dirac fermions on a triangular lattice, Physical Review B **98**, 035126 (2018).
[32] S. Sorella, Y. Otsuka, and S. Yunoki, Universal quantum criticality in the metal-insulator transition of two-dimensional interacting Dirac electrons, Physical Review X **6**, 011029 (2016), arXiv:1510.08593 [cond-mat, physics:hep-lat].
[33] S. Yin, G.-Y. Huang, C.-Y. Lo, and P. Chen, Kibble-Zurek Scaling in the Yang-Lee Edge Singularity, Physical Review Letters **118**, 065701 (2017).
[34] S. Yin, P. Mai, and F. Zhong, Universal short-time quantum critical dynamics in imaginary time, Physical Review B **89**, 144115 (2014).
[35] Y.-R. Shu, S.-K. Jian, and S. Yin, Nonequilibrium Dynamics of Deconfined Quantum Critical Point in Imaginary Time, Physical Review Letters **128**, 090601 (2022).
[36] S. Zhang, S. Yin, and F. Zhong, Generalized dynamic scaling for quantum critical relaxation in imaginary time, Physical Review E **90**, 042104 (2014).
[37] Y.-R. Shu and S. Yin, Short-imaginary-time quantum critical dynamics in the j-q 3 spin chain, Physical Review B **102**, 104425 (2020).
[38] R.-Z. Huang and S. Yin, Kibble-Zurek mechanism for a one-dimensional incarnation of a deconfined quantum critical point, Physical Review Research **2**, 033175 (2020).
[39] P. C. Hohenberg and B. I. Halperin, Theory of dynamic

critical phenomena, Rev. Mod. Phys. **49**, 435 (1977).
[40] Z.-X. Li, S. Yin, and Y.-R. Shu, Imaginary-time quantum relaxation critical dynamics with semi-ordered initial states, Chin. Phys. Lett. **40**, 037501 (2023).
[41] S. Liu, S.-X. Zhang, C.-Y. Hsieh, S. Zhang, and H. Yao, Probing many-body localization by excited-state variational quantum eigensolver, Phys. Rev. B **107**, 024204 (2023).
[42] H. Bernien, S. Schwartz, A. Keesling, H. Levine, A. Omran, H. Pichler, S. Choi, A. S. Zibrov, M. Endres, M. Greiner, V. Vuletic, and M. D. Lukin, Probing many-body dynamics on a 51-atom quantum simulator, Nature **551**, 579 (2017).
[43] S. Peotta, F. Brange, A. Deger, T. Ojanen, and C. Flindt, Determination of dynamical quantum phase transitions in strongly correlated many-body systems using loschmidt cumulants, Phys. Rev. X **11**, 041018 (2021).
[44] S.-N. Sun, M. Motta, R. N. Tazhigulov, A. T. Tan, G. K.-L. Chan, and A. J. Minnich, Quantum computation of finite-temperature static and dynamical properties of spin systems using quantum imaginary time evolution, PRX Quantum **2**, 010317 (2021).
[45] V. Janković and J. Vučičević, Fermionic-propagator and alternating-basis quantum monte carlo methods for correlated electrons on a lattice, The Journal of Chemical Physics **158**, 044108 (2023).
[46] M. Motta, C. Sun, A. T. K. Tan, M. J. ORourke, E. Ye, A. J. Minnich, F. G. S. L. Brandao, and G. K.-L. Chan, Determining eigenstates and thermal states on a quantum computer using quantum imaginary time evolution, Nature Physics **16**, 205 (2020).
[47] H. Nishi, T. Kosugi, and Y.-i. Matsushita, Implementation of quantum imaginary-time evolution method on nisq devices by introducing nonlocal approximation, npj Quantum Information **7**, 85 (2021).
[48] L. Tarruell, D. Greif, T. Uehlinger, G. Jotzu, and T. Esslinger, Creating, moving and merging dirac points with a fermi gas in a tunable honeycomb lattice, Nature **483**, 302 (2012).
[49] D. Greif, G. Jotzu, M. Messer, R. Desbuquois, and T. Esslinger, Formation and dynamics of antiferromagnetic correlations in tunable optical lattices, Phys. Rev. Lett. **115**, 260401 (2015).
[50] M. Prüfer, P. Kunkel, H. Strobel, S. Lannig, D. Linnemann, C.-M. Schmied, J. Berges, T. Gasenzer, and M. K. Oberthaler, Observation of universal dynamics in a spinor Bose gas far from equilibrium, Nature **563**, 217 (2018).
[51] J. R. Schrieffer and P. A. Wolff, Relation between the anderson and kondo hamiltonians, Phys. Rev. **149**, 491 (1966).
[52] N. Hatano and M. Suzuki, Finding exponential product formulas of higher orders, in *Quantum Annealing and Other Optimization Methods*, edited by A. Das and B. K. Chakrabarti (Springer Berlin Heidelberg, Berlin, Heidelberg, 2005) pp. 37–68.
[53] F. F. Assaad, M. Imada, and D. J. Scalapino, Charge and spin structures of a $d_{x^2-y^2}$ superconductor in the proximity of an antiferromagnetic mott insulator, Phys. Rev. B **56**, 15001 (1997).
[54] S. Sorella and E. Tosatti, Semi-metal-insulator transition of the hubbard model in the honeycomb lattice, Europhysics Letters **19**, 699 (1992).
[55] Y.-R. Shu, S. Yin, and D.-X. Yao, Universal short-time quantum critical dynamics of finite-size systems, Physical Review B **96**, 094304 (2017).
[56] Z. Li, L. Schülke, and B. Zheng, Finite-size scaling and critical exponents in critical relaxation, Phys. Rev. E **53**, 2940 (1996).
[57] H. K. Janssen, B. Schaub, and B. Schmittmann, New universal short-time scaling behaviour of critical relaxation processes, Zeitschrift für Physik B Condensed Matter **73**, 539 (1989).
[58] M. Troyer and U.-J. Wiese, Computational complexity and fundamental limitations to fermionic quantum monte carlo simulations, Phys. Rev. Lett. **94**, 170201 (2005).
[59] B. Rosenstein, D. Li, and A. Kovner, Four-fermion theory is nontrivial in 2+1 dimensions, Physical Review Letters **70**, 648 (1993).